View metadata, citation and similar papers at core.ac.uk

brought to you by CORE

provided by Repositorio Institucional de la Universidad de Alicante

THE JOURNAL OF PHYSICAL CHEMISTRY

Universitat d'Alacant
Universidad de Alicante

Subscriber access provided by Universidad de Alicante

Article

Cleavage of the C-C Bond in the Ethanol Oxidation Reaction on Platinum. Insight From Experiments and Calculations

Adolfo Ferre-Vilaplana, Carlos Buso-Rogero, Juan M. Feliu, and Enrique Herrero

J. Phys. Chem. C, **Just Accepted Manuscript** • DOI: 10.1021/acs.jpcc.6b03117 • Publication Date (Web): 10 May 2016

Downloaded from http://pubs.acs.org on May 16, 2016

Just Accepted

"Just Accepted" manuscripts have been peer-reviewed and accepted for publication. They are posted online prior to technical editing, formatting for publication and author proofing. The American Chemical Society provides "Just Accepted" as a free service to the research community to expedite the dissemination of scientific material as soon as possible after acceptance. "Just Accepted" manuscripts appear in full in PDF format accompanied by an HTML abstract. "Just Accepted" manuscripts have been fully peer reviewed, but should not be considered the official version of record. They are accessible to all readers and citable by the Digital Object Identifier (DOI®). "Just Accepted" is an optional service offered to authors. Therefore, the "Just Accepted" Web site may not include all articles that will be published in the journal. After a manuscript is technically edited and formatted, it will be removed from the "Just Accepted" Web site and published as an ASAP article. Note that technical editing may introduce minor changes to the manuscript text and/or graphics which could affect content, and all legal disclaimers and ethical guidelines that apply to the journal pertain. ACS cannot be held responsible for errors or consequences arising from the use of information contained in these "Just Accepted" manuscripts.

ACS Publications

The Journal of Physical Chemistry C is published by the American Chemical Society. 1155 Sixteenth Street N.W., Washington, DC 20036

Published by American Chemical Society. Copyright © American Chemical Society. However, no copyright claim is made to original U.S. Government works, or works produced by employees of any Commonwealth realm Crown government in the course of their duties.

Cleavage of the C-C Bond in the Ethanol Oxidation Reaction on Platinum. Insight from Experiments and Calculations.

*Adolfo Ferre-Vilaplana[a,b], Carlos Buso-Rogero[c], Juan M. Feliu[c] and Enrique Herrero[c]**

[a]Instituto Tecnológico de Informática, Ciudad Politécnica de la Innovación, Camino de Vera s/n, E-46022 Valencia, Spain,

[b]Departamento de Sistemas Informáticos y Computación, Escuela Politécnica Superior de Alcoy, Universidad Politécnica de Valencia, Plaza Ferrándiz y Carbonell s/n, E-03801 Alcoy, Spain.

[b]Instituto de Electroquímica, Universidad de Alicante, Apdo. 99, E-03080 Alicante, Spain. Phone: +34 965909814 E-mail: herrero@ua.es

ABSTRACT: Using a combination of experimental and computational methods, mainly FTIR and DFT calculations, new insights are provided here in order to better understand the cleavage step of the C-C bond taking place during the complete oxidation of ethanol on platinum stepped surfaces. First, new experimental results pointing out that platinum stepped surfaces having (111) terraces promote the C-C bond breaking are presented. Second, it is computationally shown that the special adsorption properties of the atoms in the step are able to promote the C-C scission, provided that no other adsorbed species are present on the step, which is in agreement with the experimental results. In comparison with the (111) terrace, the cleavage of the C-C bond on the step has a significantly lower activation energy, which would provide an explanation for the observed experimental results. Finally, reactivity differences under acidic and alkaline conditions are discussed using the new experimental and theoretical evidences.

INTRODUCTION

Ethanol presents a higher energy storage density than single-carbon fuels (such as methanol or formic acid) and can be produced directly as a biofuel. In return, the complete oxidation of ethanol to water and CO_2 requires of the C-C bond cleavage. On platinum electrodes, ethanol oxidation reaction takes place through a dual path mechanism.[1-2] The desired path leads to the cleavage of the C-C bond, forming adsorbed CO which is eventually oxidized to CO_2 exchanging 12 electrons in the whole process. In the other path, acetaldehyde is produced which is subsequently oxidized to acetic acid. Acetic acid is stable upon oxidation, since it can be only oxidized to CO_2 only above 1 V at room temperatures.[3] Moreover, it can be also considered as an inhibitor of the reaction, since it is adsorbed strongly on the electrode surface as acetate in acidic media, hindering the oxidation reaction.[4-5] In any case, in the oxidation to acetic acid, only 4 electrons are exchanged, losing 2/3 of the available energy. Thus, the success of ethanol based fuel cells depends on finding efficient catalysts capable of breaking the C-C bond at low overpotentials. Under acidic conditions, the major product of the ethanol oxidation on the investigated metallic electrodes at low temperatures is acetic acid.[6] This observation implies that the cleavage of C-C bond on such electrodes is a reaction step with high activation energy. Additionally, as pH increases, the efficiency in the CO_2 formation diminishes,[7] until eventually no CO_2 is formed under alkaline conditions.[8-9] In some cases, CO_2 has been detected in alkaline media by FTIR. However, in such cases the formation of CO_2 is probably related to a severe change in the pH of the solution in the thin layer configuration required to measure the IR spectra.[10]

To understand the conditions under which the C-C bond can be broken, experimental results obtained on single crystal electrodes have provided valuable insights. First, it has been shown that the Pt(111) surface is inactive for this reaction step, since the amount of CO_2 detected can be related to the presence of defects on the electrode surface.[4] Second, and more important, it has been observed that the existence of (110) steps on the (111) terrace promote the cleavage of the C-C bond in acidic environments even at low overpotentials.[4, 11-14] Thus, stepped surfaces with (111) terraces provide a very controlled environment where the scission of the C-C bond can be studied. Using isotopically labeled ethanol, it has been possible to identify two fragments produced after the cleavage of the C-C bond at low potentials:[11-13] adsorbed CO, which is oxidized above 0.5 V to CO_2, and adsorbed CH_x. This latter fragment can be oxidized to adsorbed CO above 0.4 V and subsequently to CO_2.[15] Additionally, some of the CH_x fragments can be lost by desorption and subsequent reaction with the solvent, or even being reduced to CH_4 at potentials close to 0 V, as DEMS experiments demonstrate.[16-18] On the other hand, it is clear that the solution pH plays an important role in the outcome of the reaction, since the oxidation of ethanol on alkaline solutions yields almost exclusively acetate as final product, independently of the surface structure of the electrode.[8, 10]

In order to determine the role played by the step symmetry, adsorption properties and solution pH in the ethanol oxidation reaction on platinum stepped surfaces, new spectroelectrochemical experiments and DFT computations were carried out. The results reported here provide new insights into the proba-

ble mechanism for the cleavage of the C-C bond and the effect of the adsorbed species and pH in this process.

EXPERIMENTAL AND THEORETICAL METHODS.

Electrochemical experiments. Platinum single crystal electrodes were oriented, cut and polished from small single crystal beads (ca. 2 mm in diameter for the voltammetric experiments and *ca.* 4.5 mm for the spectroelectrochemical measurements) following the procedure described by Clavilier and co-workers.[19-20] The electrodes were cleaned by flame annealing for 30 s in an oxygen/propane flame, cooled down in a H_2/Ar atmosphere and protected with water in equilibrium with this gas mixture to prevent contamination before immersion in the electrochemical cell, as described in detail elsewhere.[20-21] The single crystal electrodes used in this work are the Pt(111) surface and stepped surfaces having (110) or (100) monoatomic steps. In table 1, the Miller indexes and the corresponding step-terrace notation is given.[22]

Table 1: Notation of the different surfaces used in this work.

Step symmetry	Step-terrace notation	Miller indices
(110)	Pt(S)[16(111)×(110)]	Pt(17,17,15)
	Pt(S)[5(111)×(110)]	Pt(332)
	Pt(S)[4(111)×(110)]	Pt(553)
(100)	Pt(S)[16(111)×(100)]	Pt(17,15,15)
	Pt(S)[5(111)×(100)]	Pt(322)
	Pt(S)[4(111)×(100)]	Pt(533)

Voltammetric experiments were carried out using a waveform generator (EG&EG PARC 175), together with a potentiostat (Amel Model 2053) and a digital recorder (eDAQ ED401). For the spectroelectrochemical measurements Nicolet 8700 spectrometer equipped with a MCT (mercury cadmium telluride) detector was used. The spetroelectrchemical cell was equipped with a CaF_2 prism beveled at 60º.[23-24] IR spectra were collected with a resolution of 8 cm^{-1} and 100 interferograms for increasing the signal-to-noise ratio. A p-polarized light was used in all the FTIR experiments. The spectra are presented as absorbance measurements ($A=-\log (R_1-R_2)/R_1$), where R_2 and R_1 are the reflectance values for the single beam spectra recorded at the sample and the reference potential, respectively. Positive bands in the spectra correspond to species formed at the sample potential, whereas negative bands are referred to species consumed. The sample spectra were collected after applying successive potential steps of 100 mV between 0.10 and 0.95 V.

Solutions were prepared using ethanol absolute (Merck p.a.), NaOH (NaOH monohydrated 99.99% Merck Suprapur®), perchloric and sulfuric acid (Merck Suprapur®), and ultrapure water (Elga Purelab Ultra 18.2 MΩ cm). Ar (N50, Air Liquide) was used for desoxygenating the solutions. All the experiments were carried out at room temperature in a three-electrode electrochemical cell. A platinum wire was used as a counter-electrode and a reversible hydrogen (N50, Air Liquide) electrode was used as a reference electrode (RHE).

Computational methods. All DFT calculations were carried out using numerical basis sets,[25] semicore pseudopotentials[26] (which include scalar relativistic effects) and the RPBE functional[27] (which was specifically developed for catalysis applications) as implemented in the Dmol^3 code [28]. Solvation effects were taken into account by the COSMO model.[29] The effects of non-zero dipole moments, in the supercells, were cancelled by means of external fields.[30] Transition states were searched for using a generalization of the linear synchronous transit method,[31] for periodic systems, combined with a quadratic synchronous transit method in a complete protocol as implemented in Dmol^3. In addition, the relevant transition states were confirmed estimating the minimum energy reaction paths, between reactants and products, by means of the nudged elastic band method.[32]

The Pt(111), Pt(553) and Pt(533) surfaces were modeled by means of periodic supercells comprising 64, 76 and 64 Pt atoms (four layers of metal atoms), respectively, and a vacuum slab of 20 Å. The bottom 32, 36 and 32 Pt atoms were frozen in their bulk crystal locations, respectively. The remaining 32, 40 and 32 Pt atoms were completely relaxed joint to the adsorbates, respectively. The shortest distance between periodic images was 11.32, 10.96 and 11.32 Å, respectively.

Optimal configurations (adsorbent/adsorbate, reactants, products and transition states) were searched for using numerical basis sets of double-numerical quality. For this phase of the calculations, the optimization convergence thresholds were set to 2.0×10^{-5} Ha for the energy, 0.004 Ha/Å for the force, and 0.005 Å for the displacement. The SCF convergence criterion was set to 1.0×10^{-5} Ha for the energy. Assuming the previously optimized configurations, reaction energies and barriers were estimated using numerical basis sets of double-numerical quality plus polarization. In this case, the SCF convergence criterion was set to 1.0×10^{-6} Ha for the energy.

An orbital cutoff radius of 4.5 Å was always used in the numerical basis set for all the atoms. Brillouin zones were always sampled, under the Monkhorst-Pack method,[33] using grids corresponding to distances in the reciprocal space of the order of 0.04 1/Å. Convergence was always facilitated introducing 0.002 Ha of thermal smearing, though total energies were extrapolated to 0°K. The value 78.54 was taken, as dielectric constant for water, in the continuous solvation model.

RESULTS AND DISCUSSION

Previous results on platinum stepped surfaces have indicated that the (110) step on the (111) terrace is very active for the cleavage of the C-C in acidic media, whereas (100) steps on the same terrace have lower activity.[11] Those results were obtained using the SPAIRS technique (single potential alteration infrared spectroscopy) in sulfuric and perchloric acid solutions.[11] In this technique, IR spectra collection was coupled with the voltammetric sweep at 2 mV s^{-1}. In order to verify those results, the FTIR spectra under the same conditions has been now recorded after applying successive potential steps of 50 mV in the positive direction from 0.1 to 0.9 V to obtain a better signal-to-noise ratio. The time required to record each spectra is ca. 60 s, which is equivalent to a scan rate of ca. 0.8 mV s^{-1}, which implies longer accumulation times the sampling potentials with respect to previous results. Figure 1 shows the FTIR spectra for four different stepped surfaces having 16 and 5 atom (111) wide terraces and (110) and (100) monoatomic steps at different potentials and using the spectrum acquired at 0.1 V as reference (for the notation of the stepped surfaces see table 1). The observed bands and associated vibrational modes are summarized in table 2. For

the Pt(17,17,15), a positive band at ca. 2050 cm^{-1} associated with linearly bonded CO is already visible at 0.2 V and grows up to a potential of 0.5 V. A diminution of the band intensity is observed at 0.6 V, coinciding with the appearance and growth of the CO_2 band. Additional bands related to the formation of acetaldehyde, acetic acid and adsorbed acetate can be detected in the spectra, as has been described elsewhere.[4, 11-13] The appearance of the CO band at low potentials indicates that the cleavage of the C-C bond takes place at those potentials. For the other three electrodes, the qualitative behavior is essentially the same, showing a high CO formation rate. In the previous experiments, the surfaces with (100) steps (in this case the Pt(17,15,15) and Pt(322)) showed lower CO accumulation below 0.5 V.[11] These differences should be attributed to the different experimental conditions. In the present experiments, the potential is maintained constant during the spectra acquisition and the acquisition time is longer than in the previous experiments, improving the signal-to-noise ratio. It should also be taken into account that the spectra measured at a given potential is the result of the accumulated species on the interface at lower potentials plus the effect of this potential to species present on the interface. The longer accumulation times in this case allows the C-C bond breaking step to proceed further than in the previous experiment. Thus, it can be concluded that the (100) steps also activate the C-C bond breaking process, but at a lower accumulation rate than that measured for the (110) steps. As will be shown later, this lower accumulation is related to a lower potential window in which the cleavage can take place.

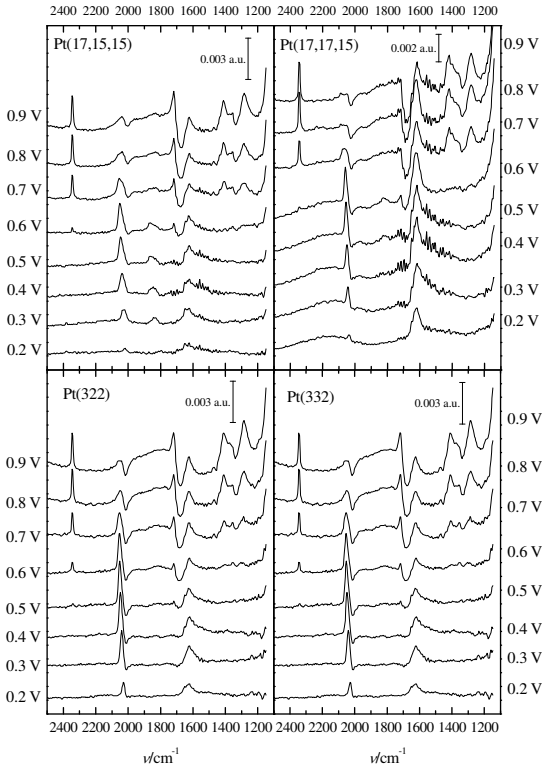

Figure 1. FTIR spectra of the different electrodes in 0.1 M HClO4+0.2 M EtOH. The reference spectrum is taken at 0.1 V.

To quantitatively analyze the results corresponding to the different stepped surfaces, the integrated band intensities for the CO_2 production and for linearly adsorbed CO (using as reference the spectra at 0.1 and 0.95 V, respectively) are plotted in figure 2. Since the integrated absorbances for the different electrodes are not directly comparable due to small changes in the thin layer configuration for each experiment, the normalized intensities with the maximum signal are represented. Several clear trends can be observed in the figure 2. First, the relative amount of CO at low potentials (E<0.3 V) is higher for the surfaces with (110) steps, as the qualitative analysis and previous experiments suggested. Second, the onset for CO_2 formation from the oxidation of adsorbed CO is displaced to negative values as the step density increases. This later result is in agreement with the catalytic role assigned to the steps (or defects) in the oxidation of adsorbed CO on (111) terraces.[34-35]

Table 2. Observed IR frequencies in the spectra for ethanol oxidation in H_2O.

υ_{H2O}/cm^{-1}	Functional group	Mode
Acidic solutions		
2340	CO_2	O-C-O asymmetric stretching
2030-2070	Adsorbed CO	Linearly bonded
1715	COOH or CHO	C=O stretching
1550	COO^-	O-C-O asymmetric stretching
1410-1420	Adsorbed -COO^-	C-O symmetric stretching
1385	-CH_3	CH_3 deformation in acetic acid
1355	-CH_3	CH_3 deformation in acetaldehyde
1280	COOH	Coupling C-O stretching + OH deformation
Alkaline solutions		
1550	-COO^-	O-C-O asymmetric stretching
1415	-COO^-	O-C-O symmetric stretching

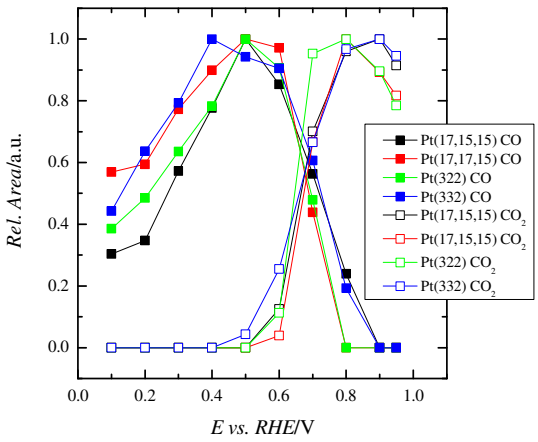

Figure 2. Integrated and normalized intensities of the CO and CO_2 bands using the spectra of figure 1. For the CO band, the reference spectrum is that acquired at 0.95 V, whereas the spectrum at 0.1 V has been used for the CO_2 band.

On the other hand, the observed behavior in alkaline solutions is completely different. As can be seen in figure 3 for the Pt(17,17,15) electrode, the only observed bands are those related to acetate, similarly to what is observed for the low index planes.[8] No adsorbed CO can be detected in the region of ca. 2050 cm^{-1}, clearly indicating that the cleavage of the C-C bond is not taking place at low potentials in this medium. The spectra for the other stepped surfaces used in this work have no significant differences with that presented in figure 3. The detection of carbonate in this media (the final oxidation product under alkaline conditions) is complicated due to the fact that the carbonate band at 1390 cm^{-1} overlaps with that related to acetate at 1415 cm^{-1}. However, the ratio between the intensity of the two bands related to acetate in the spectra (those at 1415 and 1550 cm^{-1}) is almost the same than that observed in alkaline solutions of acetate,[8] which indicates that the total formation of carbonate (if any) is very small, and that acetate is the major product of the oxidation.

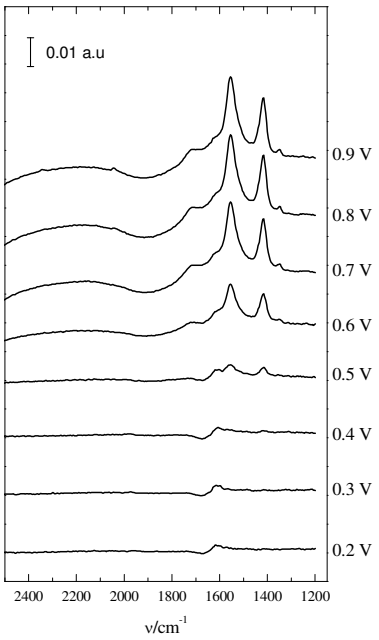

Figure 3. FTIR spectra for the Pt(17,17,15) electrode in 0.1 M NaOH+0.2 M EtOH. The reference spectrum is taken at 0.1 V.

The experimental results reported here clearly indicate that the steps in (111) terraces are key elements in the cleavage of the C-C bond in acidic solutions and that a large reactivity change occurs when pH increases. However, the voltammetric profiles of the electrodes in perchloric acid, sulfuric acid and sodium hydroxide in the absence of ethanol show only small changes (figure 4). In perchloric acid and sodium hydroxide hydrogen and OH adsorption on the (111) terraces takes place in the same potential window in the RHE scale; between 0 and 0.35 V for hydrogen and between 0.7 and 0.9 V for OH adsorption.[36] In sulfuric acid solutions, hydrogen adsorption on the (111) terraces occurs at the same potentials than in perchloric acid solution. Since the adsorption of sulfate on the (111) terrace is stronger than that of the hydroxyl anion, sulfate adsorption on the terrace gives rise to the wave that appears between 0.4 and 0.6 V. Adsorption processes on the steps give rise to a well-defined peak, whose potential depends on the step symmetry and solution pH. In acidic solutions, the peak for the steps appear at 0.13 and 0.27 V, whereas in alkaline solution, peak potentials are 0.27 and 0.42 V for the (110) and (100) steps, respectively. The process associated to the peaks clearly involved hydrogen adsorption on the steps, with a possible competition with anion adsorption (OH, or sulfate). The very small changes in the peak potential/sharpness between perchloric and sulfuric acid solution indicates that the adsorption of both anions (sulfate and hydroxyl) is weak or even not taking place and/or the adsorption strength of sulfate on the steps is very close to that of hydroxyl. On the other hand, the peak potential increase as pH increases in the RHE scale. The potential shift with pH follows a non-nernstian value of ca. 50 mV in the SHE scale per pH unit,[37] which complicates the analysis of the participant species in the peak.

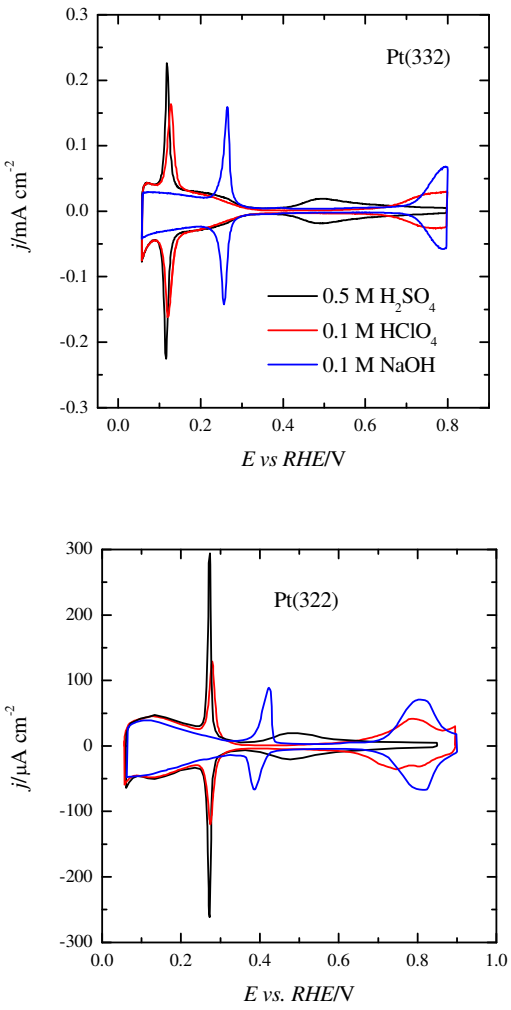

Figure 4. Voltammetric profiles of two stepped surfaces in different supporting electrolytes. Scan rate: 50 mV s^{-1}.

In order to understand the C-C bond cleavage mechanism and the effect of the surface steps, DFT calculations were carried out. Adsorbed CH_2CO bonded to two adjacent Pt atoms in an on top position (bidentate configuration) is considered as the starting point, because it has been previously proposed as the configuration from which the investigated bond cleavage would take place.[38] As has been shown, a successive reaction steps take place to reach that configuration. Those reaction steps can be summarized as follows:

$$CH_3\text{-}CH_2OH \rightarrow CH_3\text{-}{*}CHOH + H^+ + e^- \quad (1)$$

$$CH_3\text{-}{*}CHOH \rightarrow CH_3\text{-}{*}COH + H^+ + e^- \quad (2)$$

$$CH_3\text{-}{*}COH \rightarrow CH_3\text{-}{*}CO + H^+ + e^- \quad (3)$$

$$CH_3\text{-}{*}CO \rightarrow {*}CH_2\text{-}{*}CO + H^+ + e^- \quad (4)$$

where the * denotes the atom which is bonded to the surface. As can be seen, ethanol molecule is initially adsorbed through the carbon of the methoxi group. This step is followed by a series of dehydrogenation steps of this group until this part of the molecule is completely dehydrogenated. From this configuration, an additional dehydration step in the methyl group of the molecule occurs, leading to the adsorption of the species in a bidentate configuration. The C-C bond cleavage would then correspond to the step:

$$*CH_2\text{-}*CO \rightarrow *CH_2 + *CO \quad (5)$$

Evidences for this step have been found experimentally. Adsorbed CO has been directly identified in the FTIR spectra, whereas the reduction product of adsorbed CH_2, CH_4, has been detected by DEMS,[1, 7, 39] which confirms the plausibility of the considered process. From this point, these two fragments are finally oxidized to CO_2.

On the other hand, the desorption of the species from step (2), would lead to the formation of acetaldehyde,

$$CH_3\text{-}{*}COH \rightarrow CH_3\text{-}CHO \quad (6)$$

or the reaction of CH_3-*CO formed in step (4) with adsorbed OH would lead to the formation of acetic acid according to:

$$CH_3\text{-}{*}CO + {*}OH \rightarrow CH_3\text{-}COOH \quad (7)$$

Thus, the relevant steps in the compete oxidation to CO_2 are (4) and (5). Naturally, all these steps are structure sensitive, but in this study we have concentrated all the efforts in the step which has the higher activation energy, that is, step (5).[38] Additionally, our preliminary results for step (4) also indicate that the activation energy is diminished in the step.

Initial, transition and final states for the investigated bond breaking reaction step were estimated on different surfaces (Pt(111), Pt(553) and Pt(533)) and under two different reaction paths (figures 5 and 6), with the aim of determining activation barriers and energetics (Table 3 and figure 6). Under a path A, the CH_2 part of the reactant fragment moves towards the CO part, giving rise to the final state in which the CH_2 fragment rests bonded to the two initial Pt atoms and the CO fragment is bonded to the initial one and a neighboring Pt atom (figures 5 and 6 (paths A)). For path B, the CH_2 and CO parts move in opposite directions, giving rise to the final state in which the CH_2 fragment is bonded to the initial Pt atom and an additional one, whereas the CO fragment remains bonded to the initial Pt atom in on top configuration (figures 5 and 6 (paths B)). As can be observed in Table 3 and figure 6, the process energies and, especially, the energy barriers differ significantly among the different surfaces and between both paths. On the Pt(111) surface, the barriers are above 1 eV, in agreement with previous DFT calculations,[38] which suggest a very difficult cleavage of the C-C bond on this surface. Moreover, the conclusion is also in accordance with the experimental results, which show a negligible formation of CO on Pt(111) electrodes at low potentials.[4]

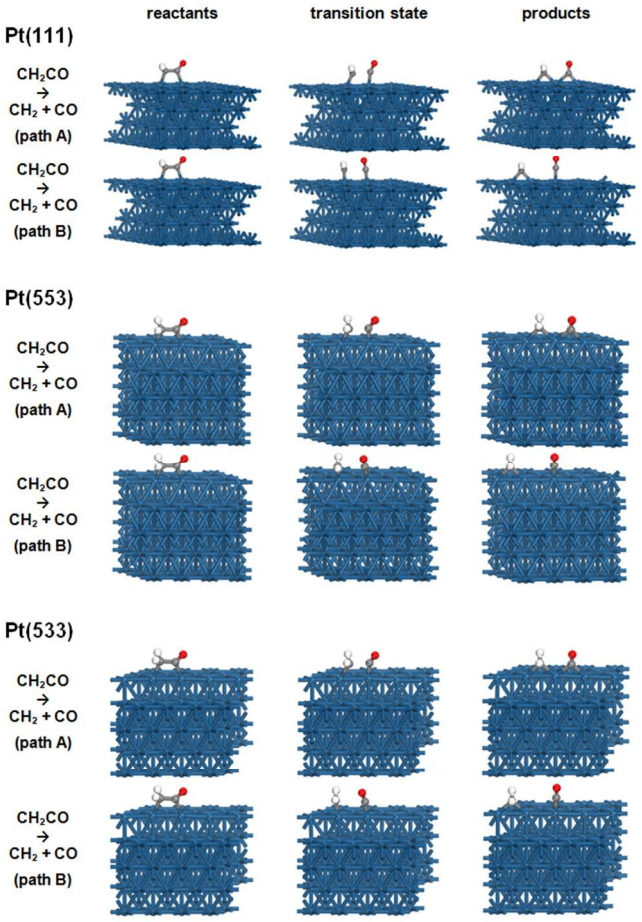

Figure 5. Initial, transition and final state for the C-C bond cleavage reaction step of adsorbed CH_2CO on the Pt(111) surface and the step of the Pt(553) and P(533) surfaces under two different paths: A (moving CH2 towards CO) and B (movig CH2 and CO in opposite directions).

However, the scene is different for the Pt(553) and Pt(533) stepped surfaces. As can be observed in figure 6 and table 3, a significant diminution of the barriers is calculated for the cleavage of the C-C bond on the steps, which is essentially the same, regardless the step symmetry. These results are in agreement with the experiments, which indicate that the steps catalyze the C-C bond cleavage. Additionally, the preferred path is always path B, since the barriers are lower (ca. 0.20-0.35 eV). This fact is probably related to the different bond energies of the CO and CH_2 fragments to the surface. In path B, the CO fragment moves to an almost on top position in the transition state to go, in the final state, to the on top position, which implies a small movement of the mass center of this fragment. However, in path A, after the transition state, a significant movement of the mass center of the CO fragment to bond the neighboring Pt atom takes place. For the CH_2 fragment, the movement is the opposite: in path A, the mass center of this fragment remains almost in the same place, whereas, for path B, a significant displacement occurs. The higher bond energy of the of the CO fragment to the surface would justify that the path with the lower barrier is that in which the CO fragment moves less from the initial position and changes less the interaction with the surface.

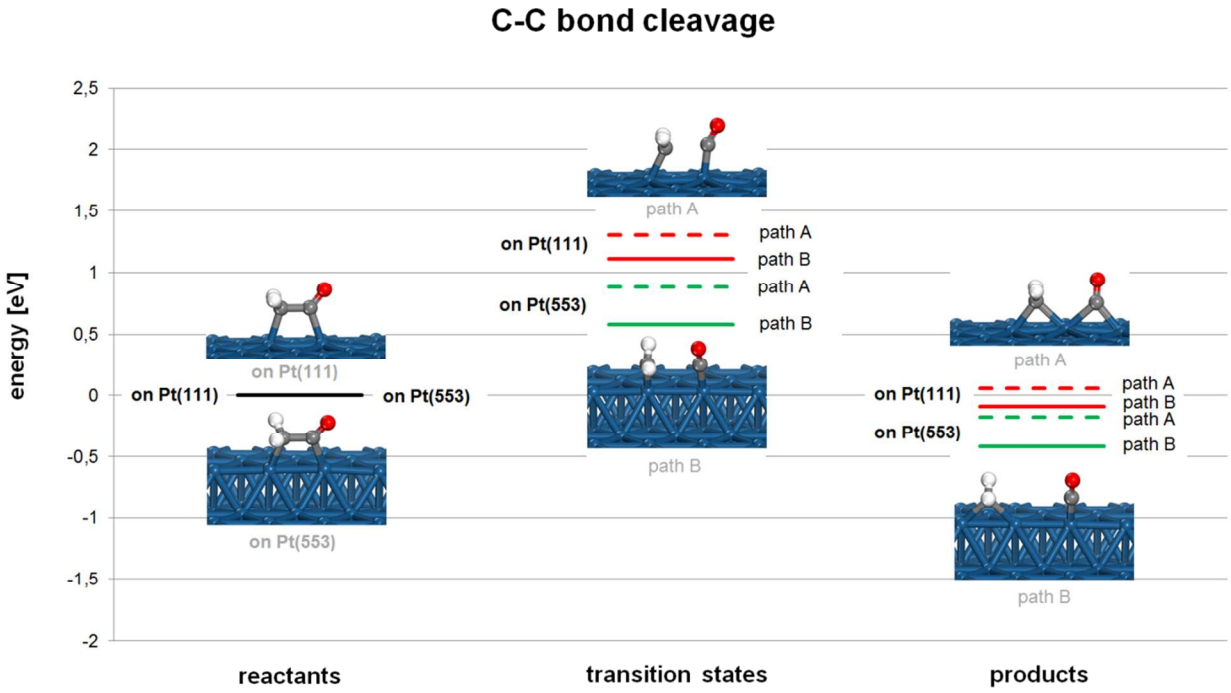

Figure 6. Energetics levels of reactants, transition states and products for the C-C bond cleavage reaction step on different surfaces and under different paths: A (moving CH_2 towards CO) and B (moving CH_2 and CO in opposite directions).

Table 3. Calculated barriers and energetics for the C-C bond cleavage reaction step on different surfaces and under different paths (see figure 5).

	Reaction step	Barrier/eV	Energy/eV
Pt(111)	$*CH_2CO \rightarrow *CO+*CH_2$ (path A)	1.30	0.06
	$*CH_2CO \rightarrow *CO+*CH_2$ (path B)	1.11	-0.09
Pt(553)	$*CH_2CO \rightarrow *CO+*CH_2$ (path A)	0.88	-0.18
	$*CH_2CO \rightarrow *CO+*CH_2$ (path B)	0.58	-0.42
Pt(533)	$*CH_2CO \rightarrow *CO+*CH_2$ (path A)	0.88	-0.54
	$*CH_2CO \rightarrow *CO+*CH_2$ (path B)	0.53	-0.67

These DFT results would explain the activity of the steps in acid solution. Moreover, they would help to understand the observed differences in the reactivity between steps of different symmetry. At very negative potentials, close to hydrogen evolution, steps are covered by hydrogen, and adsorbed hydrogen prevents an effective adsorption of ethanol. The amount of CO formed at those potentials is low. When the potential corresponding to the voltammetric peaks of the steps is reached, hydrogen is desorbed and ethanol can more easily interact with the surface, adsorbing in a bidentate position and yielding adsorbed CO and CH_2. Thus, the increase in the CO coverage for the stepped surfaces follows the peak potential, and CO formation on the surfaces with (100) steps is delayed ca. 100-150 mV with that observed for (110) stepped surfaces. The smaller potential window in which the cleave takes place for the (100) steps, justifies the differences between the previous FTIR results and these presented here.

This reactivity model implies that at potentials positive to the peak associated to hydrogen adsorption on the steps, anions (OH or sulfate) are not adsorbed on the steps, since they would prevent the adsorption and cleavage of the C-C bond. In this sense, DFT calculations show that partial OH coverages, although they allow adsorption of ethanol in a bidentate position, also increase the energy barriers to the C-C scission to values close to 1 eV, similar to those obtained for the Pt(111) terrace. Additionally, FTIR experimental results in acidic solutions indicate that at potentials above 0.4 V, the cleavage of the C-C bond is also taking place,[4] since CO is already detected at those potentials in the negative scan direction. All these evidences are in agreement with a very weak or even negligible anion adsorption on the steps.

Additionally, the identified C-C bond breaking mechanism can help to understand the very different observed reactivity in alkaline solution. In this media, steps are not active for the C-C bond cleavage. The change from acidic to alkaline media alters the charge of the electrode surface and the water structure, which can have an effect on the adsorbed species, altering the adsorption mode and strength. In alkaline solutions, the peak corresponding to the step shifts to positive values in the RHE scale, and thus, if the behavior was the same as that observed in acidic solutions, it would be expected that the potential at which CO is formed would also shift to positive values. However, no adsorbed CO or carbonate species are effectively detected. Two possible reasons could be given to explain those differences: either some species are strongly adsorbed on the steps at potentials positive to the peak potential preventing ethanol adsorption or the change in pH modi-

fies the adsorption mode of ethanol so that ethanol cannot be adsorbed in a bidentate mode.

Although other explanations have been proposed,[37] a recent study indicates that the voltammetric peak for the steps is only due to the hydrogen adsorption process, without the competing adsorption of other anions.[40] Thus, displacement of the peak to more positive potentials in the RHE scale should be attributed to the effects of the water structure/electrode charge. This interpretation is in agreement with the theoretical calculations and experimental results presented here, since the presence of any adsorbed species on the step would hinder the cleavage of the C-C bond. Thus, the most probable explanation for the differences between acidic and alkaline media is that the pH, that is, the surface charge of the electrode and water structure, significantly affects the adsorption modes of ethanol, preventing the adsorption in a bidentate position. This implies that the same effect that is displacing the peak for the steps in figure 3 is also affecting the ethanol oxidation reaction. In this respect, it should be reminded that ethanol is a very weak acid (pKa close to 14), and as the pH increases, the formation of EtO^- is facilitated. This fact could favor the adsorption of ethanol through the oxygen atom, preventing the formation of the bidentate adsorbed species, which is required for the cleavage of the C-C bond. Additionally, a high yield for CO_2 production has been found for ethanol oxidation reactions using anion exchange membranes as electrolytes,[41] which suggests that water has a relevant role in the adsorption process.

CONCLUSIONS

The experimental and computational results reported here indicate that steps on (111) terraces play a very important role in the cleavage of the C-C bond. On the one side, the activation energy for this process on the steps would be significantly lower than that on the (111) terrace. On the other side, the investigated cleavage mechanism imposes two conditions: the step should be free from other adsorbates and ethanol should be adsorbed in a bidentate arrangement through the carbons. Both observations would contribute to explain the experimental results. In acidic media, the cleavage takes place only at potentials where adsorbed hydrogen has been desorbed from the step. In alkaline media, it has been proposed that ethanol is preferentially adsorbed through the oxygen, which prevents the cleavage, justifying the absence of CO and CO_2/carbonate formation in these solutions.

AUTHOR INFORMATION

Corresponding Author

*e-mail: herrero@ua.es

Author Contributions

The manuscript was written through contributions of all authors. All authors have given approval to the final version of the manuscript.

Notes

The authors declare no competing financial interests.

ACKNOWLEDGMENT

This work has been financially supported by the MINECO (Spain) (project CTQ2013-44083-P) and Generalitat Valenciana (project PROMETEOII/2014/013).

REFERENCES

1. Iwasita, T.; Pastor, E., A Dems and Ftir Spectroscopic Investigation of Adsorbed Ethanol on Polycrystalline Platinum *Electrochim. Acta* **1994,** *39*, 531-537.
2. Shin, J. W.; Tornquist, W. J.; Korzeniewski, C.; Hoaglund, C. S., Elementary Steps in the Oxidation and Dissociative Chemisorption of Ethanol on Smooth and Stepped Surface Planes of Platinum Electrodes. *Surf. Sci.* **1996,** *364*, 122-130.
3. Rodes, A.; Pastor, E.; Iwasita, T., An Ftir Study on the Adsorption of Acetate at the Basal Planes of Platinum Single-Crystal Electrodes. *J. Electroanal. Chem.* **1994,** *376*, 109-118.
4. Colmati, F.; Tremiliosi-Filho, G.; Gonzalez, E. R.; Berna, A.; Herrero, E.; Feliu, J. M., Surface Structure Effects on the Electrochemical Oxidation of Ethanol on Platinum Single Crystal Electrodes. *Faraday Discuss.* **2008,** *140*, 379-97; discussion 417-37.
5. Prieto, M. J.; Tremiliosi-Filho, G., The Influence of Acetic Acid on the Ethanol Electrooxidation on a Platinum Electrode. *Electrochem. Commun.* **2011,** *13*, 527-529.
6. Koper, M. T. M.; Lai, S. C. S.; Herrero, E., Mechanisms of the Oxidation of Carbon Monoxide and Small Organic Molecules at Metal Electrodes. In *Fuel Cell Catalysis, a Surface Science Approach*, Koper, M. T. M., Ed. John Wiley & Sons, Inc: Hoboken, NJ, 2009; pp 159-208.
7. Busó-Rogero, C.; Brimaud, S.; Solla-Gullon, J.; Vidal-Iglesias, F. J.; Herrero, E.; Behm, R. J.; Feliu, J. M., Ethanol Oxidation on Shape-Controlled Platinum Nanoparticles at Different Phs: A Combined in Situ Ir Spectroscopy and Online Mass Spectrometry Study. *J. Electroanal. Chem.* **2016,** *763*, 116-124.
8. Busó-Rogero, C.; Herrero, E.; Feliu, J. M., Ethanol Oxidation on Pt Single-Crystal Electrodes: Surface-Structure Effects in Alkaline Medium. *ChemPhysChem* **2014,** *15*, 2019-2028.
9. Bayer, D.; Berenger, S.; Joos, M.; Cremers, C.; Tübke, J., Electrochemical Oxidation of C2 Alcohols at Platinum Electrodes in Acidic and Alkaline Environment. *Int. J. Hydrogen Energy* **2010,** *35*, 12660-12667.
10. Christensen, P. A.; Jones, S. W. M.; Hamnett, A., In Situ Ftir Studies of Ethanol Oxidation at Polycrystalline Pt in Alkaline Solution. *J. Phys. Chem. C* **2012,** *116*, 24681-24689.
11. Colmati, F.; Tremiliosi, G.; Gonzalez, E. R.; Berna, A.; Herrero, E.; Feliu, J. M., The Role of the Steps in the Cleavage of the C-C Bond During Ethanol Oxidation on Platinum Electrodes. *Phys. Chem. Chem. Phys.* **2009,** *11*, 9114-9123.
12. Souza-Garcia, J.; Herrero, E.; Feliu, J. M., Breaking the C-C Bond in the Ethanol Oxidation Reaction on Platinum Electrodes: Effect of Steps and Ruthenium Adatoms. *ChemPhysChem* **2010,** *11*, 1391-1394.
13. Del Colle, V.; Souza-Garcia, J.; Tremiliosi, G.; Herrero, E.; Feliu, J. M., Electrochemical and Spectroscopic Studies of Ethanol Oxidation on Pt Stepped Surfaces Modified by Tin Adatoms. *Phys. Chem. Chem. Phys.* **2011,** *13*, 12163-12172.
14. Tarnowski, D. J.; Korzeniewski, C., Effects of Surface Step Density on the Electrochemical Oxidation of Ethanol to Acetic Acid. *J. Phys. Chem. B* **1997,** *101*, 253-258.
15. Lai, S. C. S.; Kleyn, S. E. F.; Rosca, V.; Koper, M. T. M., Mechanism of the Dissociation and Electrooxidation of Ethanol and Acetaldehyde on Platinum as Studied by Sers. *J. Phys. Chem. C* **2008,** *112*, 19080-19087.
16. Bittins-Cattaneo, B.; Wilhelm, S.; Cattaneo, E.; Buschmann, H. W.; Vielstich, W., Intermediates and Products of Ethanol Oxidation on Platinum in Acid Solution. *Berichte der Bunsengesellschaft für physikalische Chemie* **1988,** *92*, 1210-1218.
17. Schmiemann, U.; Müller, U.; Baltruschat, H., The Influence of the Surface Structure on the Adsorption of Ethene, Ethanol and Cyclohexene as Studied by Dems. *Electrochim. Acta* **1995,** *40*, 99-107.
18. Wang, H.; Jusys, Z.; Behm, R. J., Ethanol Electrooxidation on a Carbon-Supported Pt Catalyst: Reaction Kinetics and Product Yields. *J. Phys. Chem. B* **2004,** *108*, 19413-19424.
19. Clavilier, J.; Armand, D.; Sun, S. G.; Petit, M., Electrochemical Adsorption Behaviour of Platinum Stepped Surfaces

in Sulphuric Acid Solutions *J. Electroanal. Chem.* **1986,** *205*, 267-277.
20. Korzeniewski, C.; Climent, V.; Feliu, J. M., Electrochemistry at Platinum Single Crystal Electrodes. In *Electroanalytical Chemistry: A Series of Advances*, Bard, A. J.; Zoski, C., Eds. CRC Press: Boca Raton, 2012; Vol. 24, pp 75-169.
21. Rodes, A.; Elachi, K.; Zamakhchari, M. A.; Clavilier, J., Hydrogen Probing of Step and Terrace Sites on Pt(S)-[N(111) × (100)]. *J. Electroanal. Chem.* **1990,** *284*, 245-253.
22. Lang, B.; Joyner, R. W.; Somorjai, G. A., Low Energy Electron Diffraction Studies of Chemisorbed Gases on Stepped Surfaces of Platinum. *Surf. Sci.* **1972,** *30*, 454-474.
23. Iwasita, T.; Nart, F. C.; Vielstich, W., An Ftir Study of the Catalytic Activity of a 85:15 Pt:Ru Alloy for Methanol Oxidation. *Ber. Bunsen-Ges. Phys. Chem.* **1990,** *94*, 1030.
24. Rodes, A.; Pérez, J. M.; Aldaz, A., Vibrational Spectroscopy. In *Handbook of Fuel Cells - Fundamentals, Technology and Applications*, Vielstich, W.; Lamm, A.; Gasteiger, H. A., Eds. John Wiley & Sons, Ltd: Chichester, 2003; Vol. 2.
25. Delley, B., An All-Electron Numerical Method for Solving the Local Density Functional for Polyatomic Molecules. *J. Chem. Phys.* **1990,** *92*, 508-517.
26. Delley, B., Hardness Conserving Semilocal Pseudopotentials. *Phys. Rev. B* **2002,** *66*, 155125.
27. Hammer, B.; Hansen, L. B.; Nørskov, J. K., Improved Adsorption Energetics within Density-Functional Theory Using Revised Perdew-Burke-Ernzerhof Functionals. *Phys. Rev. B* **1999,** *59*, 7413-7421.
28. Delley, B., From Molecules to Solids with the Dmol(3) Approach. *J. Chem. Phys.* **2000,** *113*, 7756-7764.
29. Delley, B., The Conductor-Like Screening Model for Polymers and Surfaces. *Mol. Simul.* **2006,** *32*, 117-123.
30. Neugebauer, J.; Scheffler, M., Adsorbate-Substrate and Adsorbate-Adsorbate Interactions of Na and K Adlayers on Al(111). *Phys. Rev. B* **1992,** *46*, 16067-16080.
31. Halgren, T. A.; Lipscomb, W. N., The Synchronous-Transit Method for Determining Reaction Pathways and Locating Molecular Transition States. *Chem. Phys. Lett.* **1977,** *49*, 225-232.
32. Henkelman, G.; Jónsson, H., Improved Tangent Estimate in the Nudged Elastic Band Method for Finding Minimum Energy Paths and Saddle Points. *J. Chem. Phys.* **2000,** *113*, 9978-9985.
33. Monkhorst, H. J.; Pack, J. D., Special Points for Brillouin-Zone Integrations. *Phys. Rev. B* **1976,** *13*, 5188-5192.
34. Lebedeva, N. P.; Koper, M. T. M.; Herrero, E.; Feliu, J. M.; van Santen, R. A., Co Oxidation on Stepped Pt N(111) X (111) Electrodes. *J. Electroanal. Chem.* **2000,** *487*, 37-44.
35. Lebedeva, N. P.; Koper, M. T. M.; Feliu, J. M.; van Santen, R. A., Role of Crystalline Defects in Electrocatalysis: Mechanism and Kinetics of Co Adlayer Oxidation on Stepped Platinum Electrodes. *J. Phys. Chem. B* **2002,** *106*, 12938-12947.
36. Rizo, R.; Sitta, E.; Herrero, E.; Climent, V.; Feliu, J. M., Towards the Understanding of the Interfacial Ph Scale at Pt(111) Electrodes. *Electrochim. Acta* **2015,** *162*, 138-145.
37. van der Niet, M. J. T. C.; Garcia-Araez, N.; Hernández, J.; Feliu, J. M.; Koper, M. T. M., Water Dissociation on Well-Defined Platinum Surfaces: The Electrochemical Perspective. *Catal. Today* **2013,** *202*, 105-113.
38. Kavanagh, R.; Cao, X.-M.; Lin, W.-F.; Hardacre, C.; Hu, P., Origin of Low Co2 Selectivity on Platinum in the Direct Ethanol Fuel Cell. *Angew. Chem. Int. Ed.* **2012,** *51*, 1572-1575.
39. Abd-El-Latif, A. A.; Mostafa, E.; Huxter, S.; Attard, G.; Baltruschat, H., Electrooxidation of Ethanol at Polycrystalline and Platinum Stepped Single Crystals a Study by Differential Electrochemical Mass Spectrometry. *Electrochim. Acta* **2010,** *55*, 7951-7960.
40. Gómez-Marín, A. M.; Feliu, J. M., Thermodynamic Properties of Hydrogen–Water Adsorption at Terraces and Steps of Pt(111) Vicinal Surface Electrodes. *Surf. Sci.* **2016,** *646*, 269-281.
41. Rao, V.; Hariyanto; Cremers, C.; Stimming, U., Investigation of the Ethanol Electro-Oxidation in Alkaline Membrane Electrode Assembly by Differential Electrochemical Mass Spectrometry. *Fuel Cells* **2007,** *7*, 417-423.

TOC graphic